CHAPTER IV

RESULTS AND DISCUSSION

Cloning of a partial sequence of *DFR* cDNA from *D.* Sonia cv. Earsakul

The cDNA synthesized from total RNA of *D.* Sonia cv. Earsakul flower buds (3.3–3.5 cm) was used as a template to amplify partial *DFR* cDNA in PCR reaction. Two pairs of specific primers DFR-F1 and DFR-R1 and DFR-F2 and DFR-R2 were designed based on the nucleotide sequence of *Dendrobium* hybrid *DFR* mRNA (accession no. FM209431). The primer sequences and map are shown in Table 2 and Figure 6. The amplification conditions were as follows; predenaturation at 92°C for 2 min, followed by 35 cycles of amplification (92°C for 30 sec, 50°C for 20 sec, 72°C for 30 sec) and then a final extension at 72°C for 5 min. RT-PCR using pairs of *DFR* primers F1-R1, F1-R2, F2-R1 and F2-R2 generated approximately 485-, 499-, 456- and 470-bp fragments, respectively (Figure 7). These fragment sizes were corresponded to the expected sizes on the nucleotide sequence of *DFR* mRNA (accession no. FM209431). The 470 bp of *DFR* candidate was isolated and cloned into pGEM-TEasy vector for DNA sequence analysis.

Table 2 Primer combinations for isolation of partial *DFR* cDNA of *D.* Sonia cv. Earsakul by RT-PCR.

Forward primer (5'-3')	Reverse primer (5'-3')	Expected PCR product size (bp)
DFR-F1: 5'GACCCTGAGAATGAAGTG3'	**DFR -R1:** 5'GAAGAGCAAATGTATCTACC3'	485
DFR-F1: 5'GACCCTGAGAATGAAGTG3'	**DFR -R2:** 5' CTGTGGAGTCATAGGAAG3'	499
DFR -F2: 5'CAATCAACGGTCTGCTGG3'	**DFR -R1:** 5'GAAGAGCAAATGTATCTACC3'	456
DFR -F2: 5'CAATCAACGGTCTGCTGG3'	**DFR -R2:** 5' CTGTGGAGTCATAGGAAG3'	470

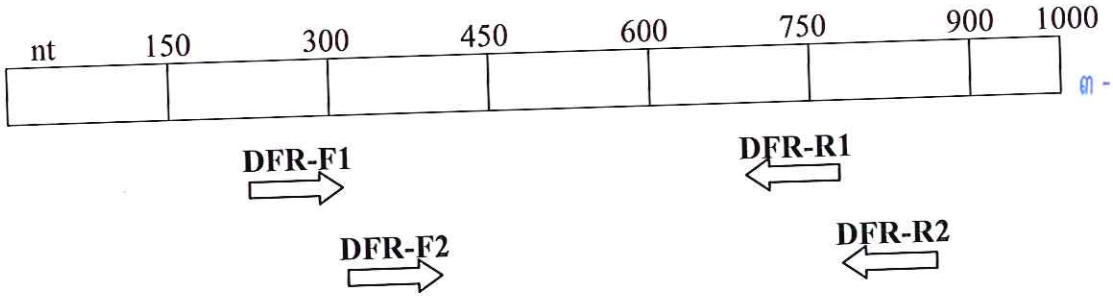

Figure 6 The physical map of *DFR* primers located on the *DFR* cDNA of *Dendrobium* hybrid cultivar (accession no. FM209431)

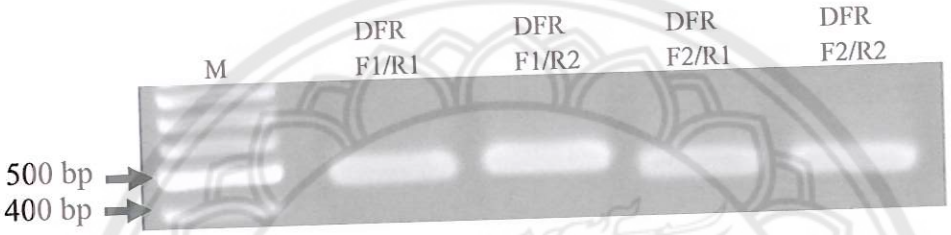

Figure 7 The *DFR* candidate of *D.* Sonia cv. Earsakul derived from RT-PCR using four different primer combinations

Note: RT-PCR using pairs of *DFR* primers F1-R1, F1-R2, F2-R1 and F2-R2 generated approximately 485-, 499-, 456- and 470-bp fragments, respectively. Lane M is 100 bp DNA Ladder.

The 470 bp *DFR* candidate clones were sequenced and analyzed using blastn (www.ncbi.nlm.nih.gov/blast). The blastn result showed that the *DFR* candidate sequence had 99%, 95% and 88% nucleotide identity to *DFR* mRNA sequence of *Dendrobium* hybrids, *D. moniliforme* and *Oncidium* sp., respectively (Table 3). This result confirmed that the isolated 470 bp PCR product was a segment of the *DFR* gene of *D.* Sonia cv. Earsakul.

Table 3 Blastn analysis of the 470 bp *DFR* candidate nucleotide sequence.

DFR candidate fragment size (bp)	Homology from blastn analysis		
	Orchid species	GenBank accession	Nucleotide identity
470	*Dendrobium* Geeting Fragrance	FJ426271	99% (431/433)
	Dendrobium Red bull	FM209432	99% (431/433)
	Dendrobium Sonia 'Earsakul'	FM209431	99% (430/434)
	Dendrobium moniliforme	HQ412559	95% (410/433)
	Oncidium sp. 'Sharry Baby'	JQ928173	88% (323/366)

Expression profiles of the *DFR* gene in *D.* Sonia cv. Earsakul flowers

The expression levels of the *DFR* gene were investigated in the sepals and petals of *D.* Sonia cv. Earsakul at seven different developmental stages (Figure 8a). RT-PCR analysis showed that the expression patterns of *DFR* in the sepals and petals during flower development were obviously different. In the sepals, the *DFR* transcripts were detected in very small amounts at stage 1, and increased with flower development to the maximum level at stage 4. The expression levels declined to undetectable levels at stage 6 (opening) and 7 (fully opened) (Figure 8b). A different temporal expression pattern was observed in petals in that the expression level of the *DFR* transcripts was prominent at stage 1, gradually accumulating to the maximum level at stage 4, with a dramatic decrease in *DFR* transcripts observed in stage 6, and an undetectable level of *DFR* transcripts noted in the fully-opened flower stage (Figure 8c). This indicated that the *DFR* expression in the sepals and petals of *D.* Sonia cv. Earsakul was developmentally regulated. A similar expression pattern of the *DFR* gene has been reported in flowers of *Torenia hybrida* (Ueyama, et al., 2002), *Gentiana triflora* (Nakatsuka, et al., 2005), *Dendrobium* hybrid (Mudalige-Jayawickrama, et al., 2005), *Petunia hybrida* (Saito, et al., 2006), *Nierembergia* sp.(Ueyama, et al., 2006), *Dendrobium* Sonia cv. Earsakul (Pitakdantham, et al., 2011), and *Ascocenda* spp. (Kunu, et al., 2012). Our results also showed that up-regulation of the *DFR* expression in the petals of *D.* Sonia cv. Earsakul started earlier than in the sepals. These expression patterns corresponded to the anthocyanin pigmentation which was initially

observed in P1 and S2. In contrast, down-regulation of *DFR* expression in the petals occurred later than in the sepals. This regulation was in accordance with the pigment intensity which appeared in the petals more strongly than in the sepals of the fully-opened flower. These observations suggest that expression of *DFR* mRNA is under developmental regulation in floral tissues.

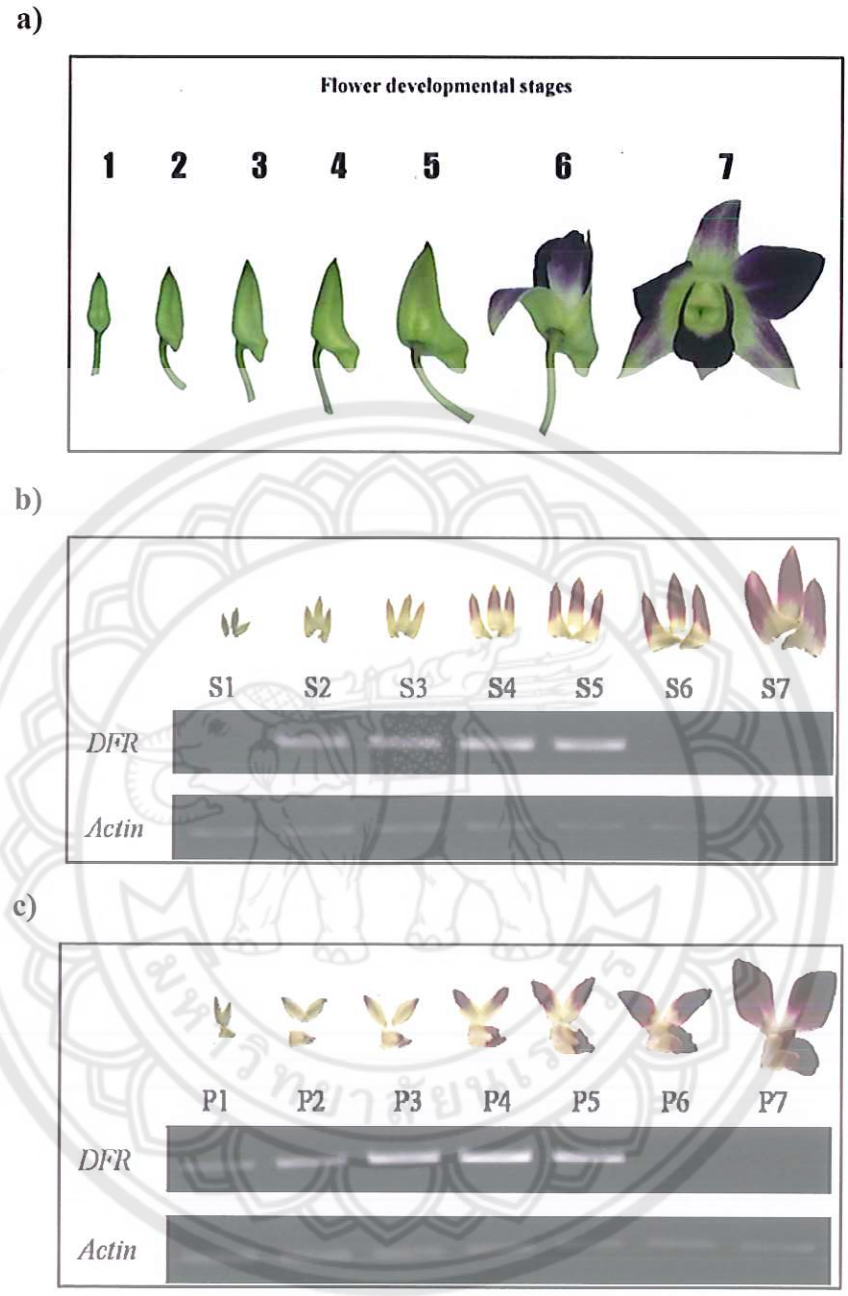

Figure 8 RT-PCR analysis of DFR expression in D. Sonia cv. Earsakul sepals and petals during flower development

Note: (a) Seven developmental stages of flowers, (b) Expression levels of *DFR* gene in sepals at seven developmental stages and (c) Expression levels of *DFR* gene in petals at seven developmental stages. *Actin* was amplified as an internal control.

To investigate the tissue specificity of the *DFR* transcripts, the total RNA from the purple and white tissues of the petals was isolated separately. RT-PCR analysis was carried out at flower bud stages 3, 4 and 5. The *DFR* transcripts were not detected in the white tissues of petals from flower bud stage 3 and were detected in small amounts in the white tissues of petals from flower bud stages 4 and 5. In the purple tissues of petals, the *DFR* transcripts were detected in all stages but the levels significantly increased from stage 3 to stages 4 and 5 (Figure 9). Semi-quantitative analysis of the *DFR* expression levels in the white and purple tissues of the petals of *D.* Sonia cv. Earsakul flower buds suggested that the white tissues would be the result of a block in the anthocyanin biosynthetic pathway at DFR. Ma, et al. (2009) also reported that the white flower of *Phalaenopsis amabilis* had a very low expression of *DFR* whereas Liew, et al. (1998) reported that *DFR* expression was detected in the red and white regions of the *Bromheadia finlaysoniana* flower. In *Petunia hybrida* cultivar Baccara Rose Picotee, the transcripts of *DFR* were detected in the white margin of the corolla at the same level as in the colored tissue whereas *CHS* transcripts were only detectable in the colored tissue (Saito, et al., 2006). *CHS* repression was also found in the white sectors of the flower of *Petunia hybrid* cultivar Red Star (Koseki, et al., 2005). These indicate that white tissues of flowers could be regulated at either earlier or later steps of the anthocyanin biosynthetic pathway. We concluded that the purple and white tissues of the *D.* Sonia cv. Earsakul petal are attributed to differential regulation of the *DFR* expression starting from early stages of the petal development. The expression of *DFR* in the purple and white tissues corresponds to the levels of anthocyanin accumulation.

Analysis of anthocyanin accumulation in the petals of *D.* Sonia cv. Earsakul

To determine the anthocyanin accumulation in different color tissues of petals, the total anthocyanins were extracted from the purple and white tissues of petals from flower buds at stages 3, 4 and 5. In the purple tissues, anthocyanins were detected in all tested flower stages and significantly increased from stage 3 to stage 5. The anthocyanin contents were 2.5± 0.10, 6.2 ± 0.17 and 9.4± 0.56 units/g of fresh tissue from stages 3, 4 and 5, respectively (Figure 10). In the white tissues, anthocyanin accumulation was very low. The anthocyanin contents were 0.066±

0.0074, 0.076 ± 0.0045 and 0.086 ± 0.0038 units/g of fresh tissue from stages 3, 4 and 5, respectively (Figure 10). The accumulation levels of anthocyanins coincided with visible purple pigmentation.

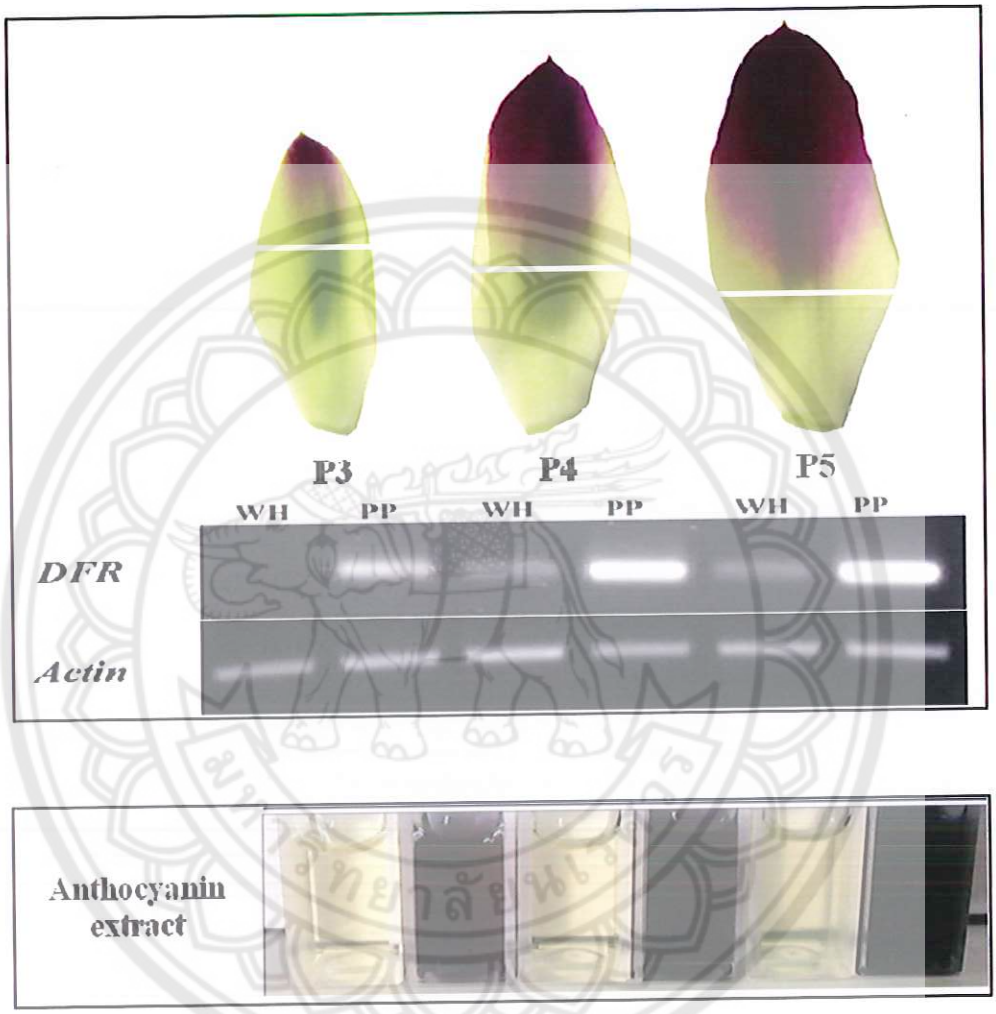

Figure 9 RT-PCR analysis of *DFR* expression and anthocyanin extracts in white and purple tissues of petals P3, P4 and P5 from flower bud stages 3, 4 and 5, respectively

Note: *Actin* was amplified as an internal control. WH and PP indicate white and purple tissues, respectively. The white bars on petals divide white and purple tissues of each stage

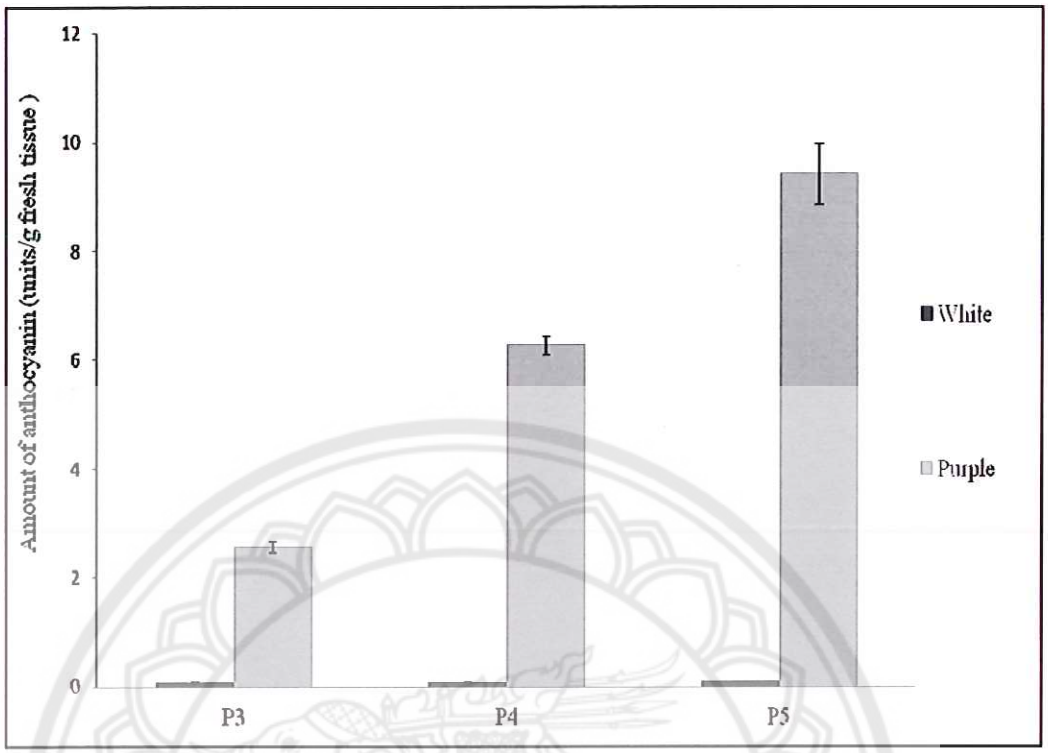

Figure 10 Quantitative analysis of anthocyanin contents in white and purple tissues of petals P3, P4 and P5 from flower bud stages 3, 4 and 5, respectively

Note: The black bar indicates the amount of anthocyanins from white tissues and the gray bar indicates the amount of anthocyanins from purple tissues. The data represents the mean and standard errors obtained from two replicates per sample

Cloning of the *DFR*-hairpin RNA binary vectors using Gateway Technology

To construct the *DFR*-hairpin RNA binary vector construct, we used Gateway Technology (Invitrogen, USA) which is a method based on the site-specific recombination of bacteriophage lambda to transfer DNA of interest from the entry vector into the expression vector. Our project used the commercial entry vector, pENTR™ 3C Dual vector (Invitrogen, USA), and the hairpin RNA expression vector, pSTARGATE and pWATERGATE provided by CSIRO, Australia.

The isolated *DFR* cDNA of *D.* Sonia cv. Earsakul was transferred from the pGEM-TEasy-*DFR* clone (pGEM-*DFR*) to pENTR™ 3C Dual vector (pENTR) by restriction enzyme cloning with *EcoRI*. Digestion of pENTR with *EcoRI* appeared 3 different bands, which were approximately 2290, 1160 and 330 bp, on 1% (w/v) TAE agarose gel electrophoresis (Figure 11a). Digestion of pGEM-*DFR* with *EcoRI* revealed 2 different bands, which were approximately 3000 and 470 bp, on 1% (w/v) TAE agarose gel electrophoresis (Figure 11b). The 3-kb band was the pGEM-TEasy vector. These bands corresponded to the *EcoRI* restriction sites on the physical map of pENTR (Appendix B). To reduce the self-ligated pENTR vector in the ligation reaction, *EcoRI* digested pENTR was treated with FastAP™ Thermosensitive Alkaline Phosphatase (Fermentas, Canada).

The purified 470 bp fragments obtained from pGEM-*DFR* digested with *EcoRI* were ligated to the purified 2290 bp pENTR backbone obtained from pENTR digested with *EcoRI*. The transformed *E. coli* strain DH5α was selected on medium containing 50 µg/ml kanamycin. The pENTR-*DFR* clone was screened by colony PCR (Figure 12a). The *EcoRI* digestion was confirmed that the selected pENTR-*DFR* clone contained the 470 bp of *DFR* fragment (Figure 12b).

To generate pSTARGATE-*DFR* and pWATERGATE-*DFR*, which were *DFR*-hairpin RNA binary vectors, the 470 bp of *DFR* fragment located in pENTR-*DFR* clone was transferred to pSTARGATE and pWATERGATE vectors using LR recombination technique as described in CHAPTER II. The products of LR recombination between pENTR-*DFR* and the expression vectors, pSTARGATE and pWATERGATE, were transformed into *E. coli* strain DH5α. The transformed cells were screened on medium containing spectinomycin. The pSTARGATE-*DFR* and pWATERGATE-*DFR* clones growing on spectinomycin were tested by colony PCR using a pair of primers DFR-F2 and DFR-R2, (Figure 13 and Figure 14). The result showed that three selected colonies of each clone contained the 470-bp *DFR* cDNA. The selected pSTARGATE-*DFR* and pWATERGATE-*DFR* clones were used for the transient RNAi silencing experiment.

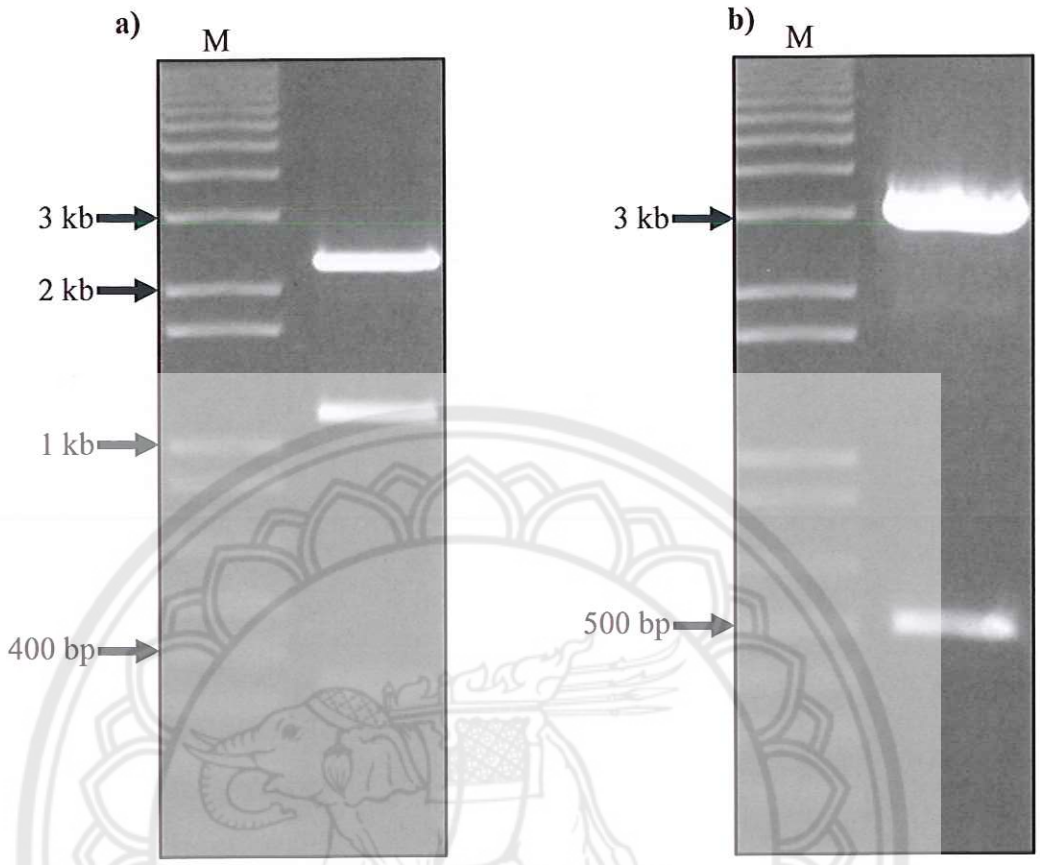

Figure 11 Digestion of pENTR and pGEM-*DFR* with *EcoRI*

Note: (a) DNA fragments, approximately 2290, 1160 and 330 bp, obtained from *EcoRI*-digested pENTR and (b) DNA fragments, approximately 3000 and 470 bp, obtained from *EcoRI* -digested pGEM-*DFR*. Lane M, 1 Kb plus DNA Ladder.

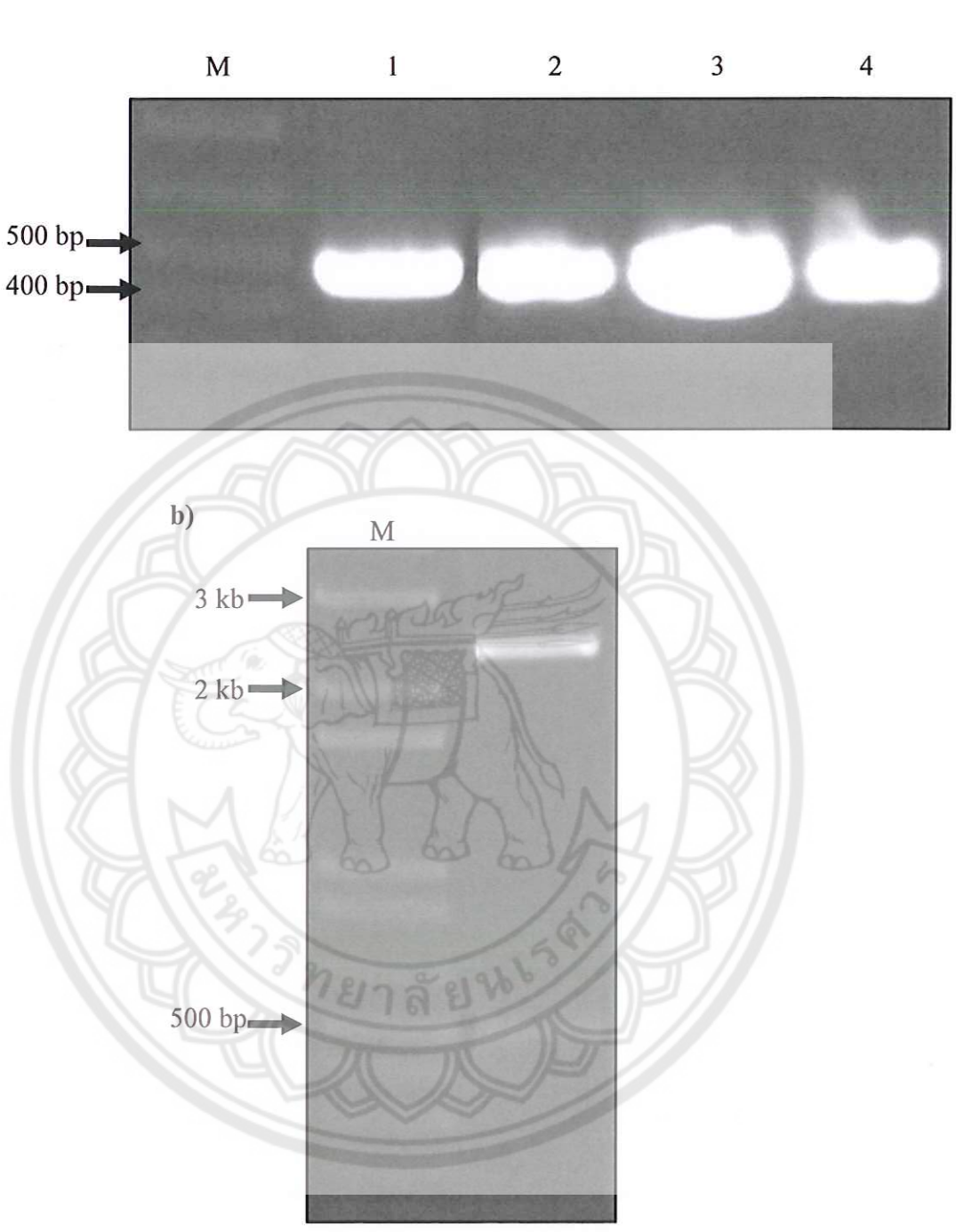

Figure 12 Analysis of pENTR-*DFR* clones

Note: (a) Colony PCR screening; lane M, 1 Kb plus DNA Ladder; lane 1, the positive control using pGEM-*DFR* plasmid as a PCR template; lane 2-4, positive colonies from kanamycin selection, (b) *Eco*RI digestion of the selected pENTR-*DFR* plasmid; lane M, 1 Kb plus DNA.

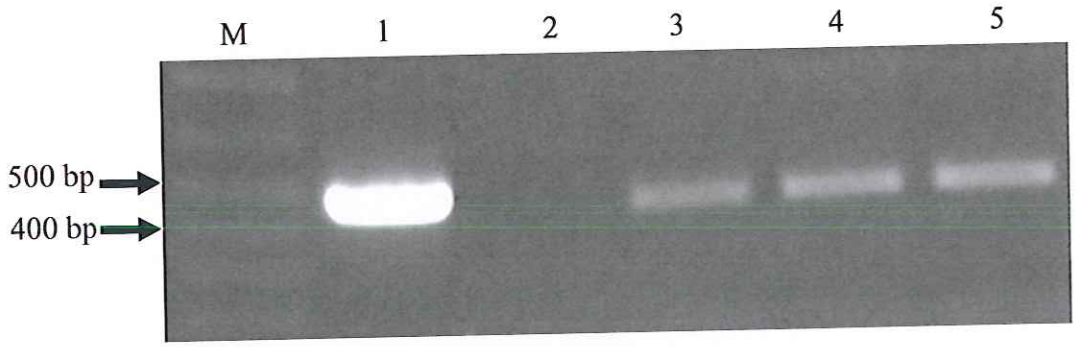

Figure 13 Analysis of pSTARGATE-*DFR* clones by colony PCR using a pair of primers *DFR*-F2 and *DFR*-R2

Note: Lane M, 1 Kb plus DNA Ladder; lane 1, the positive control using pGEM-*DFR* plasmid as a PCR template; lane 2, the negative control (PCR with no template); lane 3-5, positive colonies from spectinomycin selection.

Figure 14 Analysis of pWATERGATE-*DFR* clones by colony PCR using a pair of primers *DFR*-F2 and *DFR*-R2

Note: Lane M, 1 Kb plus DNA Ladder; lane 1, the positive control using pGEM-*DFR* plasmid as a PCR template; lane 2, negative control (PCR with no template); lane 3-5, positive colonies from spectinomycin selection.

Transient RNAi mediated *DFR* silencing by agroinfiltration in *D.* Sonia cv. Earsakul flowers

1. Development of an effective method for transient RNAi mediated *DFR* silencing in *D.* Sonia cv. Earsakul flowers

Two different methods for transient RNAi mediated *DFR* silencing in *D.* Sonia cv. Earsakul flowers using *Agrobacterium*-mediated transient transformation were performed. The first method was agroinjection on the cracked flower-bud sepals and petals and the second method was agroinfiltration on the cracked flower-bud sepals and petals. The suspension of *A. tumefaciens* strain EHA105 carrying the pSTARGATE-*DFR* and pWATERGATE-*DFR* constructs was diluted to OD600 value of 0.5 – 0.6. *Agrobacterium* cultures containing 100 μM acetosyringone were used for infection the flowers.

For agroinjection, we performed on flower bud stages 2 and 3 in which the *DFR* expression was increasing. The *Agrobacterium* suspension (approximately 0.3 ml) was needle-injected at two different sites on sepals through inside petals of flower buds attached to the flower stems on the plants. The injected flower buds attached to the flower stems on the plants were co-cultivated at 25 °C for 5 days then moved to a nursery where no temperature was controlled until the infiltrated flower buds fully opened (the experiment was carried out in December 2011 at Faculty of Agriculture, Natural Resources and Environment, Naresuan University, Phitsanulok, Thailand).

Seven days after injection, the *A. tumefaciens* strain EHA105 containing pSTARGATE-*DFR* and pWATERGATE-*DFR* injected flowers developed the small colorless regions around the injected sites of sepals and petals (Figure 15 and Figure 16). A silencing efficiency of 100% was achieved in the stage 2 and 3 injected flowers. The similar agroinjection silencing for supporting this method has been reported in flowers of *CHS* in tomato (Orzaea, et al., 2006).

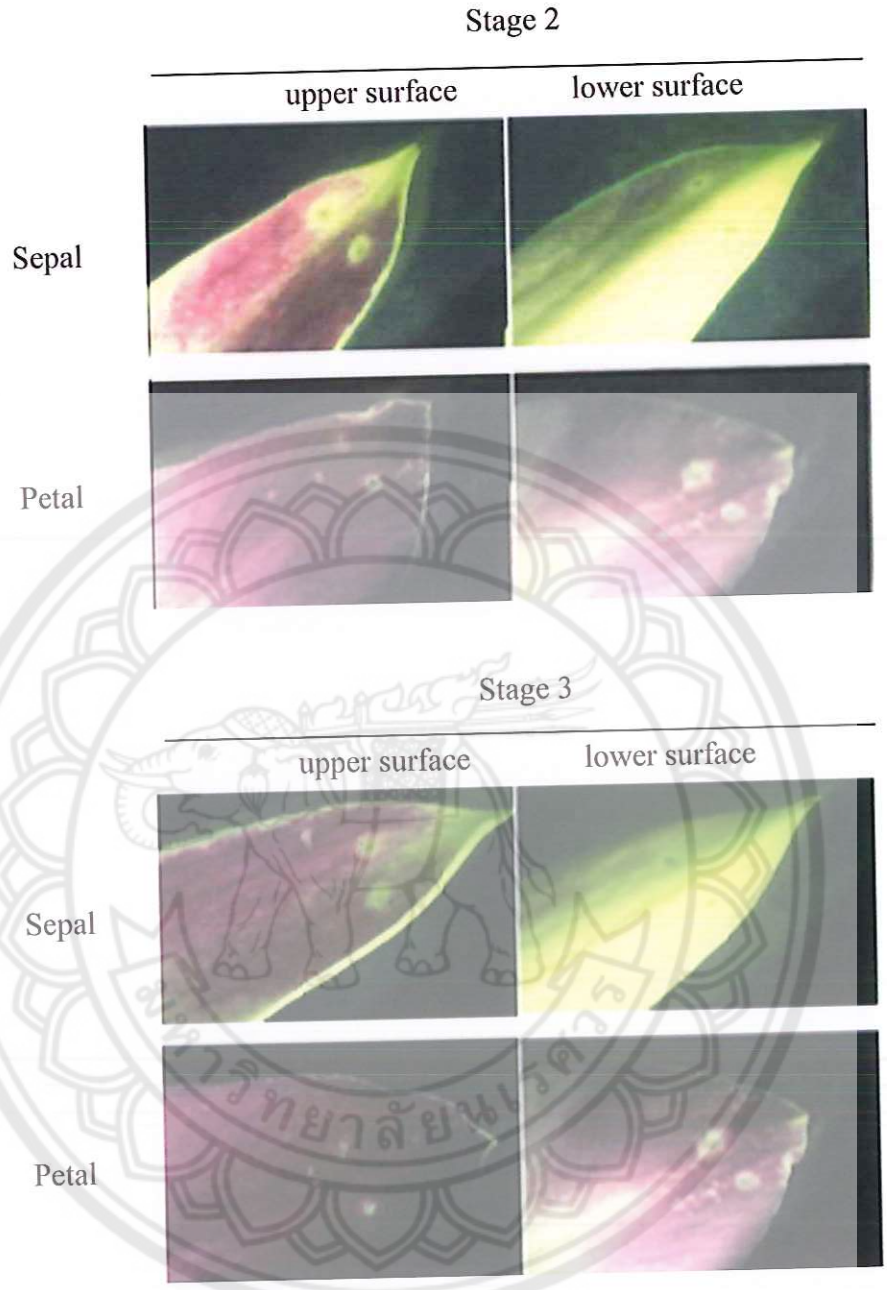

Figure 15 Silenced phenotypes of the flowers injected with *A. tumefaciens* strain EHA105 containing pSTARGATE-*DFR*

Note: Agroinjection was performed on flower bud stages 2 and 3 which still attached to the plant from backside of sepals through inside petals. Photographs of injected sepals and petals were taken at day 5 after injection.

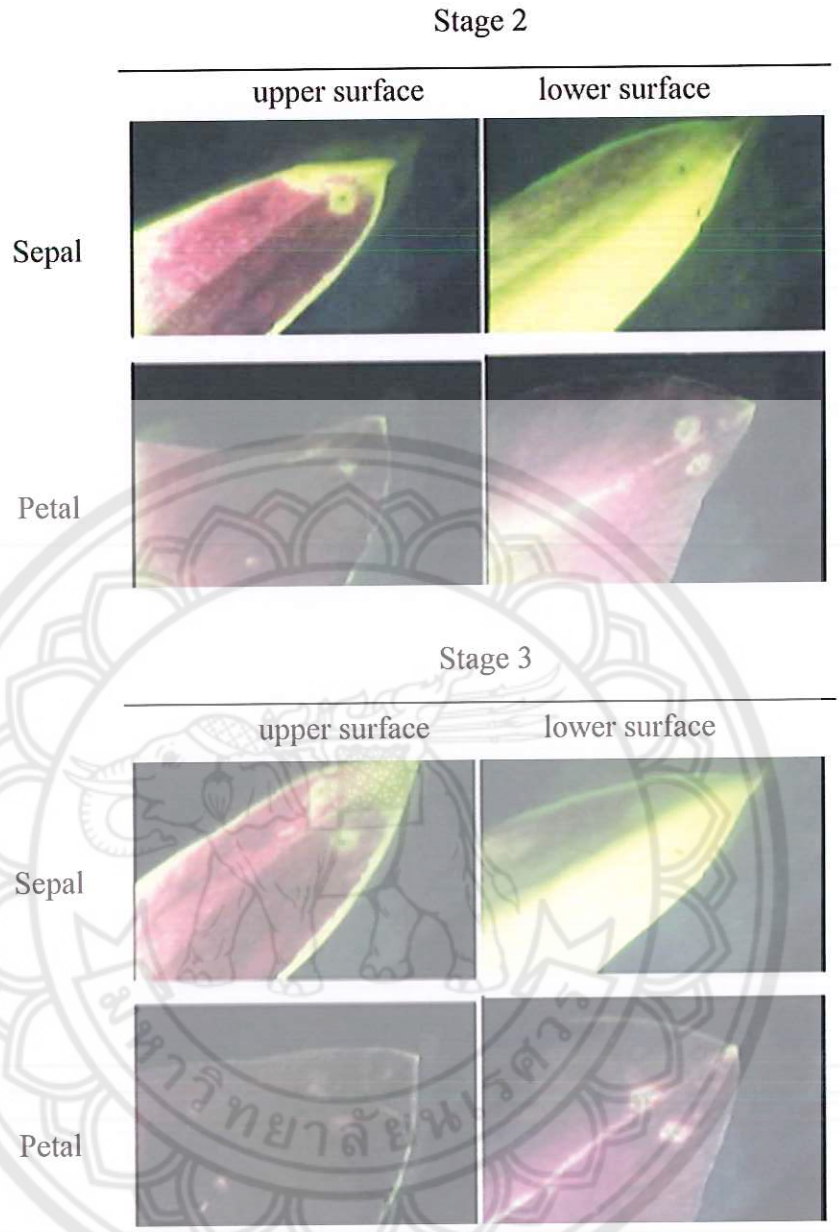

Figure 16 Silenced phenotypes of the flowers injected with *A. tumefaciens* strain EHA105 containing pWATERGATE-*DFR*

Note: Agroinjection was performed on flower bud stages 2 and 3 which still attached to the plant from backside of sepals through inside petals. Photographs of injected sepals and petals were taken at day 5 after injection.

For agroinfiltration, we also performed on flower bud stages 2, and 3 attached to the flower stems on the plants. Flower buds were cracked to open for sepals and petal infiltration. The *Agrobacterium* suspension was gently injected with needle at a single site followed by infiltration on the sepals and petals upper surface of cracked flower buds still attached to the plants. The infiltrated flowers were co-cultivated at 25 °C for 5 days and then moved to a nursery as mentioned above. Two days after infiltration (still in a co-cultivation time), the *A. tumefaciens* strain EHA105 containing pSTARGATE-*DFR* and pWATERGATE-*DFR* infiltrated sepals and petals of flower bud stages 2 and 3 started to develop colorless sectors where the inoculums were infiltrated. The colorless sectors developed as impaired anthocyanin accumulation were obviously observed in both the upper and lower surface of the sepals and petals on day 3-4 after infiltration with a silencing efficiency of 100% colorless phenotype (Figure 17 and Figure 18).

The results of two methods of *Agrobacterium*-mediated transient transformation developed for transient *DFR* RNAi in *D.* Sonia cv. Earsakul flowers showed that agroinfiltration was much more effective method than agroinjection for observation of the flower color change. The agroinfiltration method was then used as the transient RNAi silencing system in further research experiments.

To confirm the suppression of *DFR* gene at the molecular level, we performed semi-quantitative RT-PCR using a pair of primers DFR-F1 and DFR-R1 to amplify the endogenous *DFR* cDNA in the stage-2 and -3 sepals and petals infiltrated with pSTARGATE-*DFR* and pWATERGATE-*DFR*. Total RNA was extracted from the sepals and petals at day 5 after infiltration and *Actin* was used as an internal control for RT-PCR amplification. The expression levels of the endogenous *DFR* were compared between the normal color and pale color or colorless regions of the same infiltrated sepals and petals. The results revealed that the expression levels of the endogenous *DFR* at the pale color or colorless regions of all infiltrated sepals and petals were significantly lower than the normal color regions (Figure 19 and Figure 20). This indicated that both *DFR*-hpRNA constructs driven by the Ubiquitin promoter on pSTARGATE-*DFR* and by the ARbcS promoter on pWATERGATE-*DFR* effectively silenced the endogenous *DFR* expression causing inhibition of anthocyanin synthesis and accumulation.

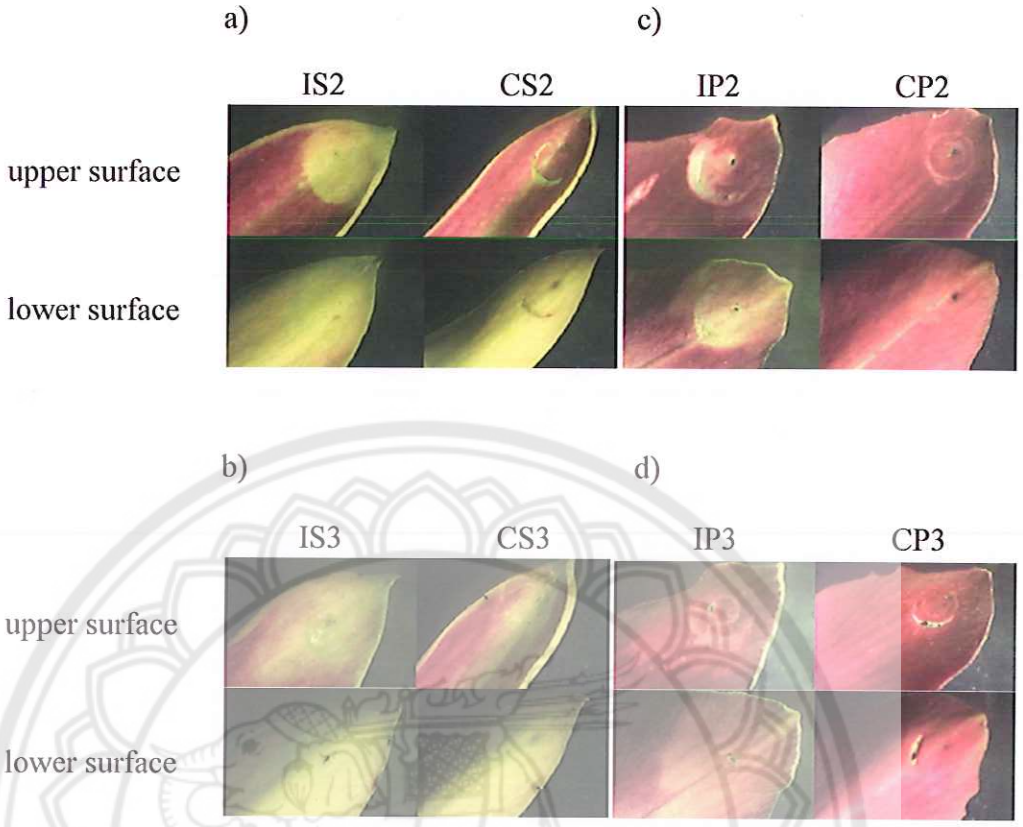

Figure 17 Silenced phynotype of the pSTARGATE-*DFR* infiltrated flowers

Note: Agroinfiltration was performed on sepals and petals upper surface of flower bud stage 2 and 3 with still attached to the inflorescence on the plant; (a) the stage-2 infiltrated sepal, (b) the stage-3 infiltrated sepal, (c) the stage-2 infiltrated petal, and (d) the stage-3 infiltrated petal; IS, the sepal infiltrated with *A. tumefaciens* strain EHA105 containing pSTARGATE-*DFR*; IP, the petal infiltrated with *A. tumefaciens* strain EHA105 containing pSTARGATE-*DFR*; CS, the sepal infiltrated with empty *A. tumefaciens* strain EHA105; CP, the petal infiltrated with empty *A. tumefaciens* strain EHA105. Photographs of infiltrated sepals and petals were taken at day 5 after infiltration.

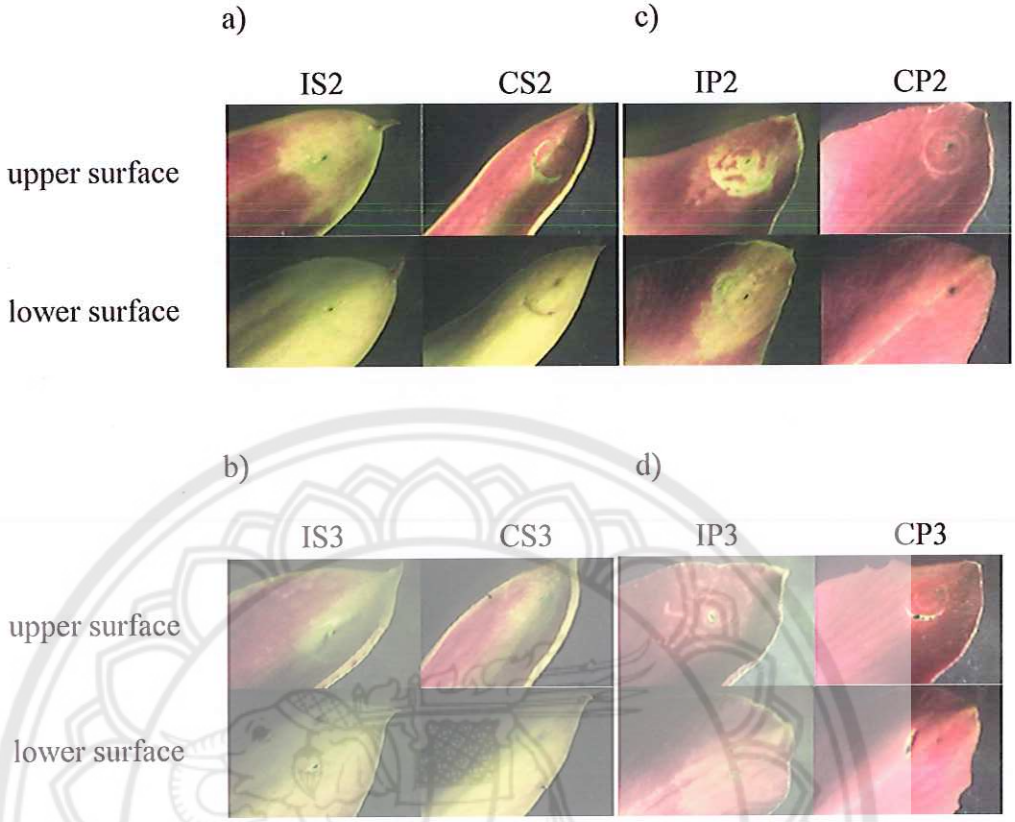

Figure 18 Silened phynotype of the pWATERGATE-*DFR* infiltrated flowers

Note: Agroinfiltration was performed on sepals and petals upper surface of flower bud stage 2 and 3 with still attached to the inflorescence on the plant; (a) the stage-2 infiltrated sepal, (b) the stage-3 infiltrated sepal, (c) the stage-2 infiltrated petal, and (d) the stage-3 infiltrated petal; IS, the sepal infiltrated with *A. tumefaciens* strain EHA105 containing pWATERGATE-*DFR*; IP, the petal infiltrated with *A. tumefaciens* strain EHA105 containing pWATERGATE-*DFR*; CS, the sepal infiltrated with empty *A. tumefaciens* strain EHA105; CP, the petal infiltrated with empty *A. tumefaciens* strain EHA105. Photographs of infiltrated sepals and petals were taken at day 5 after infiltration.

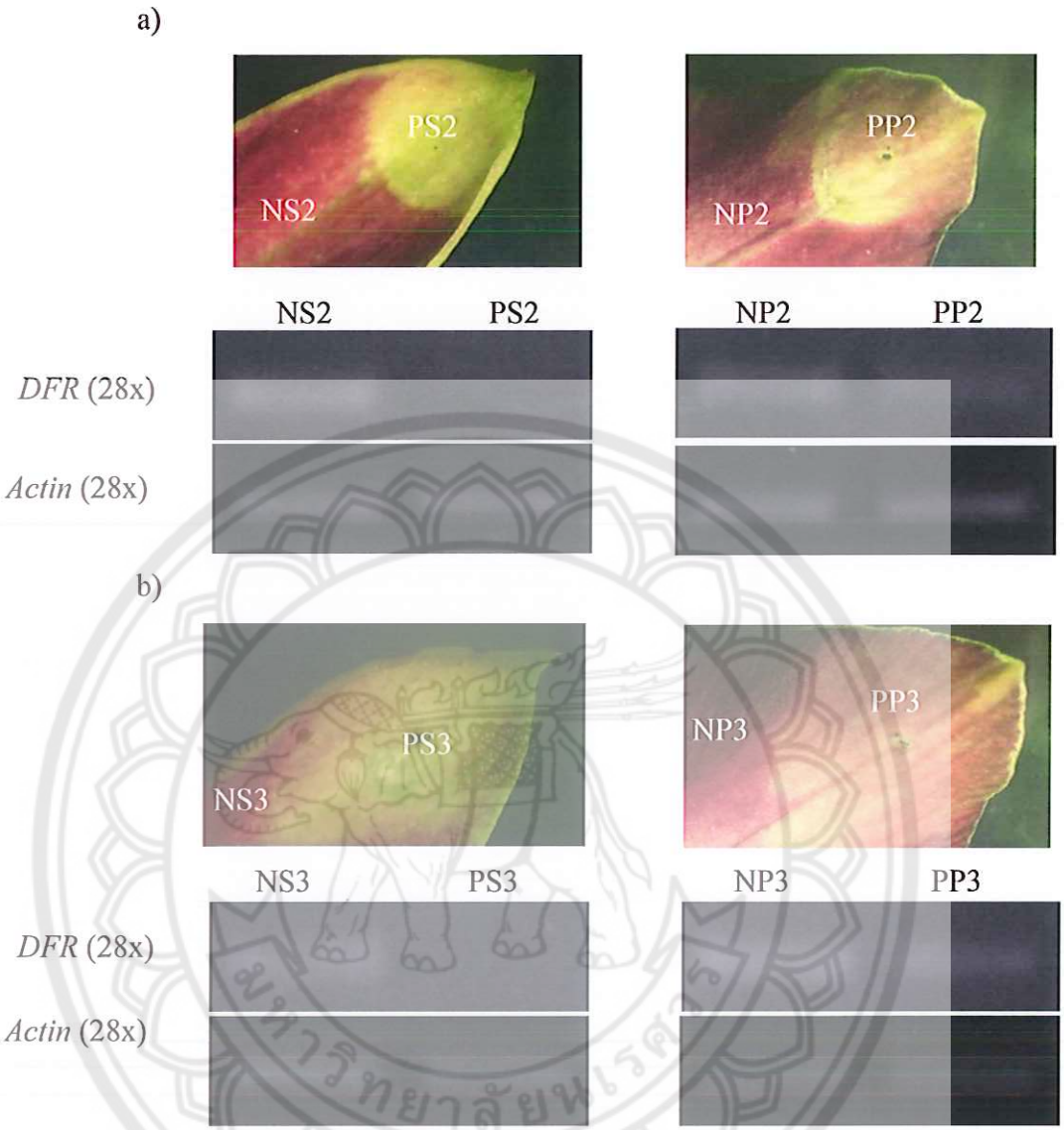

Figure 19 RT-PCR analysis of transient RNAi silencing of the *DFR* gene in the pSTARGATE-*DFR* infiltrated stage-2 and -3 sepals and petals of *D.* Sonia cv. Earsakul at day 5 after infiltration

Note: (a) pSTARGATE-*DFR* infiltrated stage-2 sepal and petal,PS2 and PP2, the pale color or colorless region of the infiltrated stage-2 sepal and petal, respectively; NS2 and NP2, the normal color region of the infiltrated stage-2 sepal and petal, respectively, (b) pSTARGATE-*DFR* infiltrated stage-3 sepal and petal, PS3 and PP3, the pale color or colorless region of the infiltrated stage-3 sepal and petal; NS3 and NP3, the normal color region of the infiltrated stage-3 sepal and petal respectively.

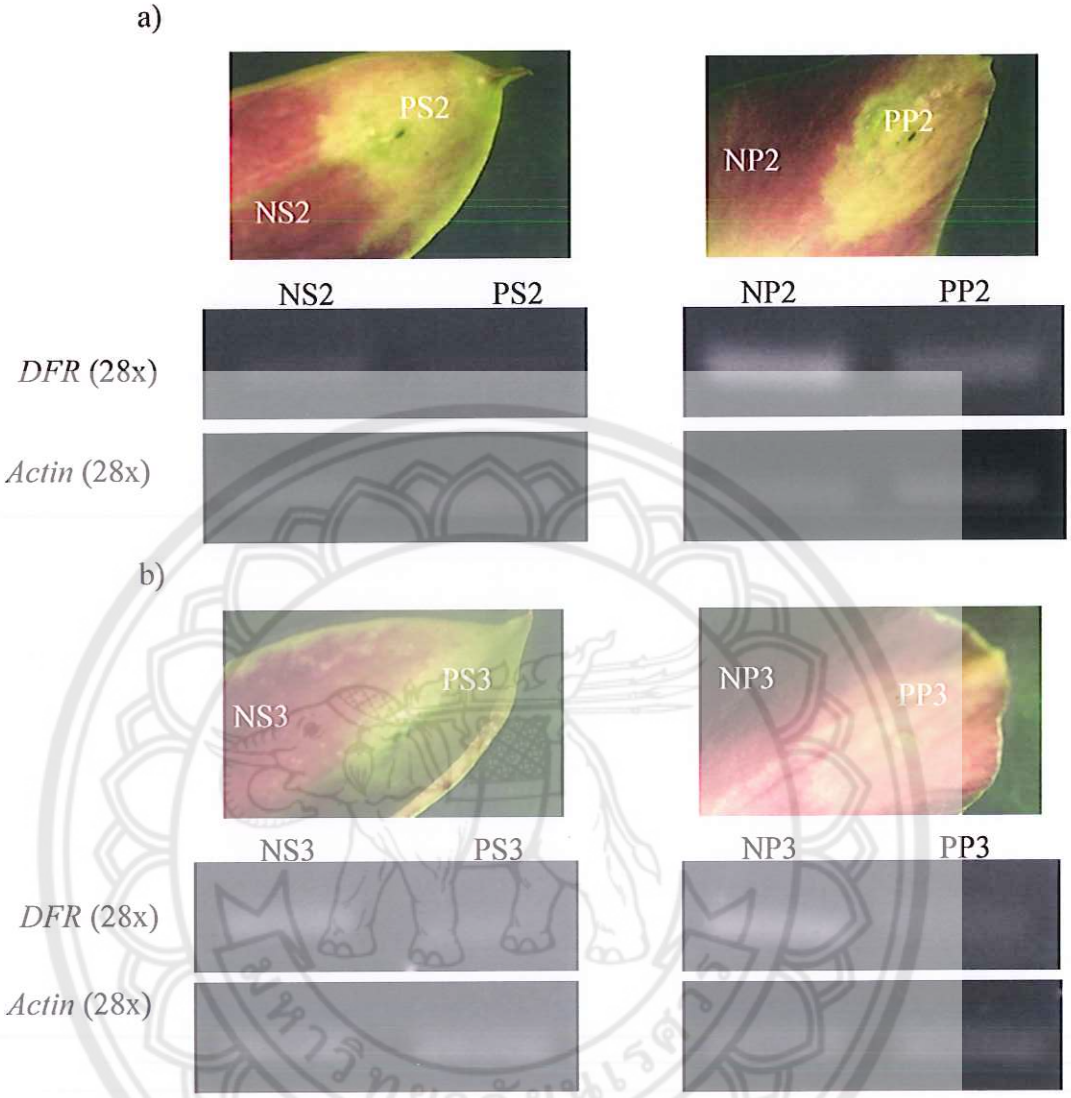

Figure 20 RT-PCR analysis of transient RNAi silencing of the *DFR* gene in the pWATERGATE-*DFR* infiltrated stage-2 and -3 sepals and petals of *D.* Sonia cv. Earsakul at day 5 after infiltration

Note: (a) pWATERGATE-*DFR* infiltrated stage-2 sepal and petal, PS2 and PP2, the pale color or colorless region of the infiltrated stage-2 sepal and petal, respectively; NS2 and NP2, the normal color region of the infiltrated stage-2 sepal and petal, respectively, (b) pWATERGATE-*DFR* infiltrated stage-3 sepal and petal, PS3 and PP3, the pale color or colorless region of the infiltrated stage-3 sepal and petal; NS3 and NP3, the normal color region of the infiltrated stage-3 sepal and petal respectively.